ELSEVIER

Journal of Alloys and Compounds 388 (2005) 266–273

Journal of ALLOYS AND COMPOUNDS

www.elsevier.com/locate/jallcom

Structure and thermal stability of ball milled Ti–Al–H powders

J. Morales-Hernández[a], J. Velázquez-Salazar[b], L. García-González[b], F.J. Espinoza-Beltrán[c,*], J.D.O. Barceinas-Sánchez[d], J. Muñoz-Saldaña[c]

[a] *Programa de Posgrado en Ingeniería, Facultad de Ingeniería, Universidad Autónoma de Querétaro, Centro Universitario Cerro de las Campanas, Col. Centro, C.P. 76000, Querétaro, Qro., México*

[b] *Programa de Posgrado en Materiales del Centro de Investigación y de Estudios Avanzados del IPN, Unidad Querétaro, Libramiento Norponiente 2000, Fracc. Real de Juriquilla, C.P. 76230, Querétaro, Qro., México*

[c] *Centro de Investigación y de Estudios Avanzados del IPN, Unidad Querétaro, Libramiento Norponiente 2000, Fracc. Real de Juriquilla, C.P. 76230, Querétaro, Qro., México*

[d] *Centro de Tecnología Avanzada del Estado de Querétaro, Calz. del Retablo 150 Col. FOVISSSTE, C.P. 76150, Querétaro, Qro., México*

Received 22 June 2004; received in revised form 26 July 2004; accepted 28 July 2004

Abstract

Powders with different compositions of the binary Ti–Al system were prepared by indirect reactive ball milling (IRBM). During milling, nanocrystalline powders of titanium and titanium–aluminium hydrides were obtained using methanol as a reactive control agent. The formation of these hydride compounds due to the reaction Ti–Al–methanol improved grain size reduction of the powders. Light metal hydrides were detected by X-ray diffraction (XRD) and thermogravimeter and differential thermal analysis (TG–DTA) techniques even after very short milling times (4 h). The use of methanol as a hydrogen source during ball milling seems to be an inexpensive and easy way to prepare nanocrystalline and amorphous ductile metal based alloys in considerably shorter milling times and without an atmosphere of hydrogen gas.

Keywords: Ti–Al alloys; High-energy ball milling; X-ray diffraction; Thermal analysis; Intermetallic compounds

1. Introduction

Ti–Al alloys have been of much interest in recent years as lightweight and as structural materials for elevated temperature strength, oxidation and corrosion resistance applications. Recently, a number of non-equilibrium and amorphous phases produced by mechanical alloying (MA) of a mixture of pure elemental powders in the solid state such as Mg–Ni have been reported [1,2]. The MA method is particularly promising for the manufacture of homogeneous metastable alloys such as amorphous alloys and supersaturated solid solutions [1] enhancing in most of the cases mechanic, catalytic and thermodynamic properties. Several compositions of the binary Ti–Al system have been already produced by MA [3,4]. For instance, Ti–Al alloys with high Al content milled in argon atmosphere for times as long as 1000 h to reach the nanometric particle size and amorphous state, have been reported [5,6]. The agglomeration of the elemental powders can be significantly reduced by introducing of TiH_2 powders as a process control agent (PCA) in the MA process, which reduces the milling time (in one order of magnitude) and increases milling efficiency [2,7]. The effective particle size reduction using a hydride phase has been proven for Zr–Ni [8] and Ti–Al [9] compounds in a hydrogen atmosphere, which leads to the formation of light metal hydrides and also prevent the oxidation. The mechanism of milling is enhanced due to the brittleness behavior transferred to the powders by the introduced or formed metal hydrides. Further on, the absence of a PCA in the milling leads to a cold welding process, which inhibits the milling of the powders [2]. The removing of this PCA agent after milling does not represent a problem considering its low thermal stability (unstable at temperatures higher than 250 °C). However, the management

* Corresponding author. Tel.: +52-442-4414913; fax: +52-442-4414938.
E-mail address: fespinoza@qro.cinvestav.mx (F.J. Espinoza-Beltrán).

0925-8388/$ – see front matter © 2004 Elsevier B.V. All rights reserved.
doi:10.1016/j.jallcom.2004.07.023

of either metal hydrides or hydrogen atmospheres, to in situ form these hydrides, both as a PCA in the milling process represent a challenge due to its high reactivity when exposed to the atmosphere. This, in fact increases the necessity of use of glove boxes with controlled atmospheres even during the preparation of powders for milling.

We used a novel method to synthesize titanium–aluminum hydride by a modification of the reactive ball milling process (RBM) [10]. Our modification, which will be called hereafter indirect reactive ball milling (IRBM), consists in the replacement of the hydrogen atmosphere with a small amount of a reactive liquid (methanol) during milling, keeping argon as atmosphere. The methanol will be called the reactive process control agent (RPCA) in this procedure. A systematic study of the Ti–Al system prepared by this process of IRBM has not been reported yet.

The aim of this paper is to study the structural evolution and thermal stability of nanocrystalline and amorphous Ti–Al alloy powders obtained by IRBM process, where aluminum content was varied from 5 to 90 wt.%. In this work, results on the monitoring of formation of (Ti, Al)H brittle phases in the different compositions of Ti–Al powders are presented. The behavior of the particle sizes reduction and the formation of amorphous phases at different milling times are analyzed.

2. Experimental details

Elemental powders of Al and Ti (99.8 and 99.5% pure, respectively and average particle size 50 μm) were mixed to prepare several Ti–Al compositions ($Ti_{100-x}Al_x$, x = 8.5, 16.5, 30.7, 43.2, 72.7 *y* 94.2 at.% Al). IRBM was carried out for 4, 8, 12, 16, 24, 30 and 36 h in a SPEX 8000 Mixer/Mill. Methanol was added as RPCA. Stainless steel balls AISI-410, with diameters of 3.3 mm and 8.0 mm, were introduced in a hardened steel vial, evacuated and sealed in a glove box, which was filled with 99.9% of pure argon. The total powder weight was 8.0 g and the ball to powder ratio was 5:1. After milling procedure, the samples were kept in an argon gas atmosphere for periods longer than 12 h to reduce their reactivity with the ambient, and to use them for the several analyses, especially for mixtures with higher aluminum content.

The structure and phases content of the milled powder was examined by X-ray diffraction (XRD) (Rigaku-DMAX/1200) with Ni-filtered and Cu Kα radiation and the powder morphology by scanning electron microscopy (SEM) (XL30 ESEM Philips) operated at 20 kV. Thermogravimeter and differential thermal analysis (TG–DTA) (Mettler Toledo TGA/SDTA851e) were performed under nitrogen flow with a heating rate of 10 °C/min. The microstructure of the powders also was investigated by a transmission electron microscope (TEM) (JEOL-JEM-2000FX II).

3. Results and discussion

3.1. Powder preparation

Fig. 1 shows a series of XRD patterns indicating the evolution of phases as a function of milling time (0–16 h) of the sample Ti–8.5 at.% Al (Ti–5 wt.% Al). Before milling, the XRD pattern shows characteristic peaks from the starting elements. After 4 h of milling, aluminum atoms diffuse into Ti lattice, which can be observed in the XRD pattern by the vanishing of Al peaks. On the other hand, we observed an increasing of the Ti peaks intensity. This has been already reported as the formation of a solid solution of Al in Ti with

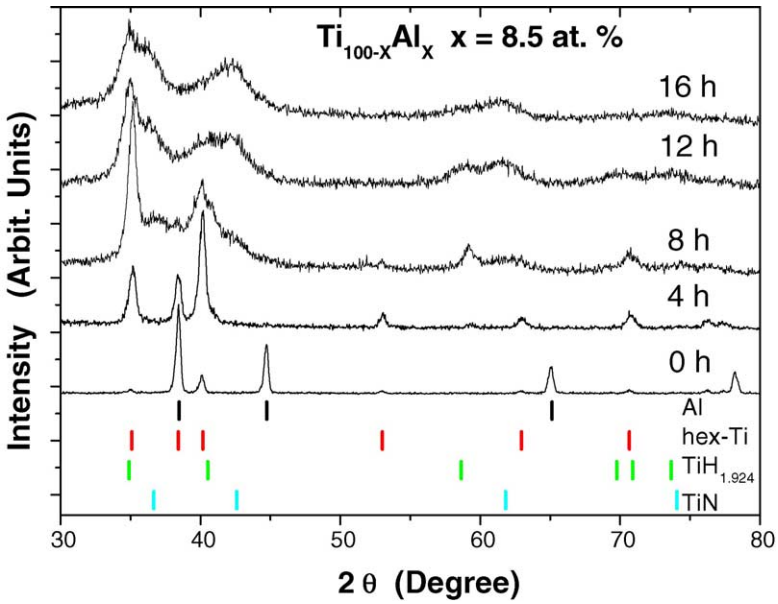

Fig. 1. XRD patterns of Ti–8.5 at.% Al (Ti–05 wt.% Al) powders ball milled by IRBM for different times until amorphous state is reached.

a structure similar to that of hex-Ti [11]. The solid solution Ti(Al) shows an asymmetric broadening with a light shifting of the XRD peaks as a function of milling time compared to the original titanium positions. The $TiH_{1.924}$ phase formation is already observed after 4 h of milling as a more intense peak at about 35° (2θ position), very close to one of the reference lines for Ti(Al) (denoted as Ti). The formation of this metal hydride must be the result of the reaction between the hydrogen arising from the RPCA with Ti(Al) in the current milling condition. This mechanochemical process is milling time dependent. As the milling time increases, this reaction leads to a gradual increasing of the relative intensity of the peak related to $TiH_{1.924}$. After 8 h of milling the main diffraction peak of the titanium hydride reaches its highest intensity, while a broadening and an intensity reduction of the XRD peaks of Ti(Al) was observed. This intensity reduction is correlated with the particle size reduction and formation of an amorphous phase. These results coincide with those reported by Itsukaichi et al. [12] for the same alloy system. It is well known that nitrogen contamination takes place after the milling procedure, when the Ti–Al powder is in an amorphous state [13] and it is exposed to the room atmosphere. Contamination with nitrogen was here observed for samples without or low aluminum content as superimposed broad and low intensity peaks of TiN with $TiH_{1.924}$. This contamination does not represent a problem and can be easily avoided by increasing either the aluminum content or the resting time in argon atmosphere of the samples. On the other hand, as mentioned before, the presence of a brittle component such as $TiH_{1.924}$, has a great contribution in the reduction of particle size and also for producing amorphous phases [8]. After 16 h of milling, a single broad peak of an amorphous phase is observed with the maximum diffraction about $2\theta \approx 42°$, and a remnant signal due to $TiH_{1.924}$, is still observed (Fig. 1). A similar behavior was observed for the samples with compositions 16.5, 30.7, and 43.2 at.% Al (not shown here). Thus, the sequence of phase transformations observed in $Ti_{100-x}Al_x$ milled samples at the compositions $x \leq 43.2$ at.% Al can be represented as follows:

$$\mathrm{Ti} + \mathrm{Al} + \mathrm{RPCA} \rightarrow \mathrm{Ti(Al)_{solid\ sol.}} + \mathrm{TiH_{1.924}} \rightarrow \mathrm{(Ti,\ Al)H_{amorphous}} + \mathrm{TiN} \quad (1)$$

Burgio et al. [14] reported the formation of an amorphous phase after long time of MA (longer than 100 h) for similar Ti–Al compositions, without PCA additions.

Fig. 2 shows the diffraction patterns for a sample with Al content of 72.7 at.% (Ti–60 wt.% Al) for the milling time values of 4, 12, 24 and 30 h. After 4 h of milling, diffraction peaks due to hex-Ti are observed as small and broad peaks, some of them coinciding with peaks of $TiH_{1.924}$. This clearly indicates that one part of the Ti content reacts with hydrogen to form titanium hydride. The main diffraction peak of Al decreases with milling time, which is due to an alloying with $TiH_{1.924}$ to form a (Ti, Al)H ternary alloy. Hashi et al. [15] reported (Ti, Al)H diffraction patterns similar to that of $TiH_{1.924}$ with a peak shifting depending on the Al content. We additionally measured the interplanar distance of the sample Ti–72.7 at.% Al. A progressive shifting of the interplanar distance of (1 1 1) $TiH_{1.924}$ peak with milling time (from 2.569 Å for 4 h to 2.575 Å for 30 h) and simultaneous decreasing of (1 1 1) Al peak intensity were observed. Both behaviors are due to the formation of (Ti, Al)H alloy. After 30 h of milling there is no evidence of grain size reduction. This is due to the high aluminum content in the sample, which inhibits the fragility effect of the hydride on the powder. We observed a similar behavior for samples with higher aluminum content (as high as 94.1 at.% Al), where the diffraction peaks

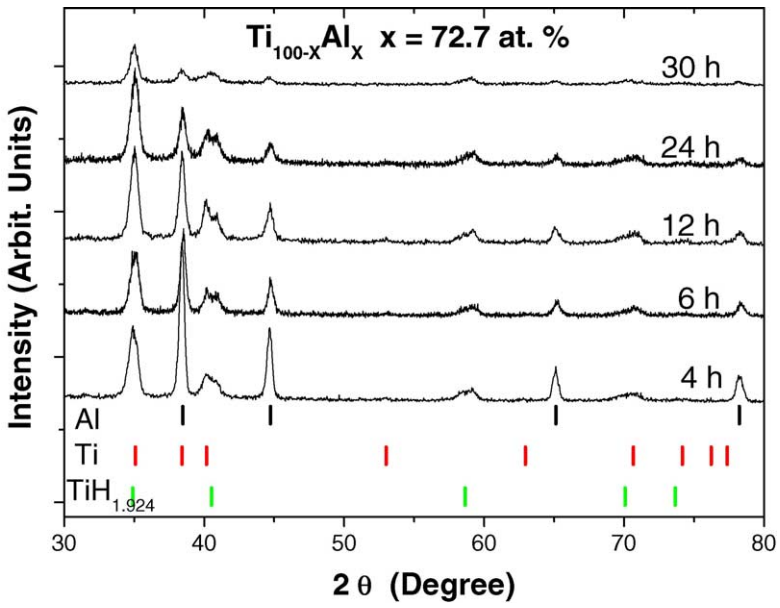

Fig. 2. XRD patterns of Ti–72.7 at.% Al (Ti–60 wt.% Al) powders ball milled by IRBM for different times until amorphous state is reached.

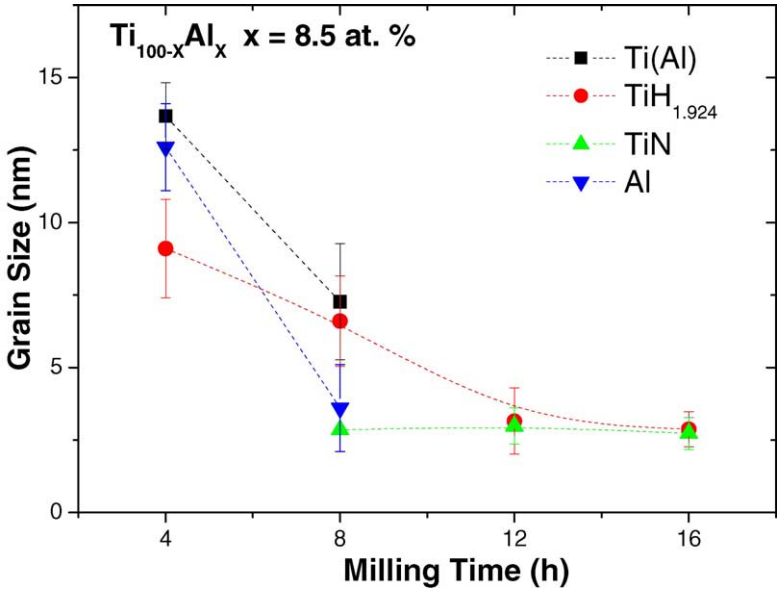

Fig. 3. Variation in grain size of Ti–8.5 at.% Al (Ti–05 wt.% Al) powders as a function of milling time in IRBM.

of $TiH_{1.924}$ phase show lower intensity. Thus, in a system with these aluminum contents, larger time periods of milling are required for an effective grain size reduction. We confirmed the existence of a compromise between brittleness of hydrides and welding of aluminum, both processes showing a strong dependence on the titanium and aluminum contents. The sequence of phase transformations for $Ti_{100-x}Al_x$ samples with compositions $x > 43.2$ at.% Al, and for long milling time (which is longer when x increases), can be represented as follows:

$$Ti + Al + RPCA \rightarrow Al(Ti)_{solid\ sol.} + (Ti, Al)H_{amorphous} \quad (2)$$

The average grain size of the IRBM milled powders was determined from XRD data by applying a profile analysis to all diffraction peaks (Ti, Al, $TiH_{1.924}$, and TiN) in accord with the Warren–Averbach method [16]. Results as a function of milling time for Ti–8.5 at.% Al (Ti–5 wt.% Al) and Ti–72.7 at.% Al (Ti–60 wt.% Al) powders are shown in Figs. 3 and 4, respectively. The advantage of using the Warren–Averbach analysis to obtain average grain size is that it proves more consistent grain size values, even for samples with XRD patterns with superimposed peaks. Nanometric grain sizes (less than 15 nm) were already attained even after 4 h ball milling, regardless of the Al content by using the

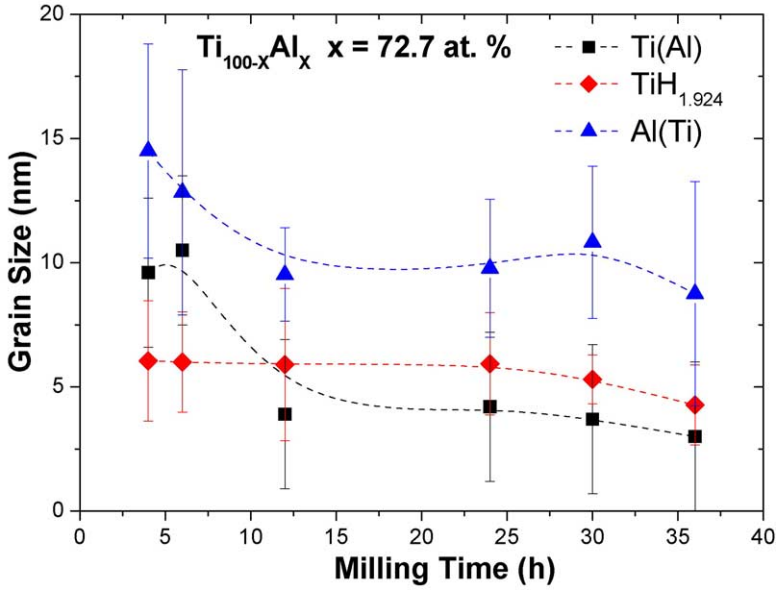

Fig. 4. Variation in grain size of Ti–72.7 at.% Al (Ti–60 wt.% Al) powders as a function of milling time in IRBM.

IRBM process. The grain size was reduced to about 7 nm after a milling time of 8 h and to about 5 nm after 12 h and approx. 3 nm after 16 h, reaching an amorphous state for powders with small amount of Al (Ti–5 wt.% Al). Again, it is important to remark the vanishing of the Al peaks from the XRD data after 8 h, which is indicative of the dissolution of Al into the Ti lattice leading to the formation of a metastable Ti(Al) solid solution before the development of the metal hydride. The measurement of grain size particularly from the TiN peaks revealed both nanocrystallites with size of less than 3 nm and powders in an amorphous state.

For compositions with high Al content (Ti–60 wt.% Al), an average grain size of less than 10 nm was measured for the Al(Ti) peaks after a milling time of 12 h and thereafter no further reduction was measured. For the same powders, the Ti(Al) and $TiH_{1.924}$ showed constant reduction in grain size as a function of milling time up to reach sizes of less than 5 nm. In general, as the Al content increases longer milling time is needed to reach particle sizes of less than 5 nm or amorphous powders. Using the IRBM process we were able to produce powders with these characteristics of the system Ti–Al by milling times as short as 16 h for alloys with low and middle Al contents and 36 h for alloys with high Al contents. As mentioned before, the main effect in the mechanism of reduction in particle size comes from the formation of a titanium hydride during milling.

Results on ball milling of the Ti–Al system were reported by different authors. For instance, Moon and Lee [17] and Moon et al. [18] prepared Al–Ti alloys with high Al-contents by conventional RBM (using hydrogen atmosphere). These authors report results of grain size as a function of the milling time between 10 and 15 nm for milling times as long as 100 h. No clear evidence on the formation of the titanium hydrides are observed from the XRD patterns, which is possibly the reason for the long milling times. In this same way, Takasaki and Fruya [19] reported results about the Ti–Al system milled in a planetary ball mill, using hydrogen atmosphere for times of about 30 h to obtain amorphous structure. In that work, the authors did not observe the formation of the hydride phase. Further on, Zhang et al. [20] studied the thermal stability

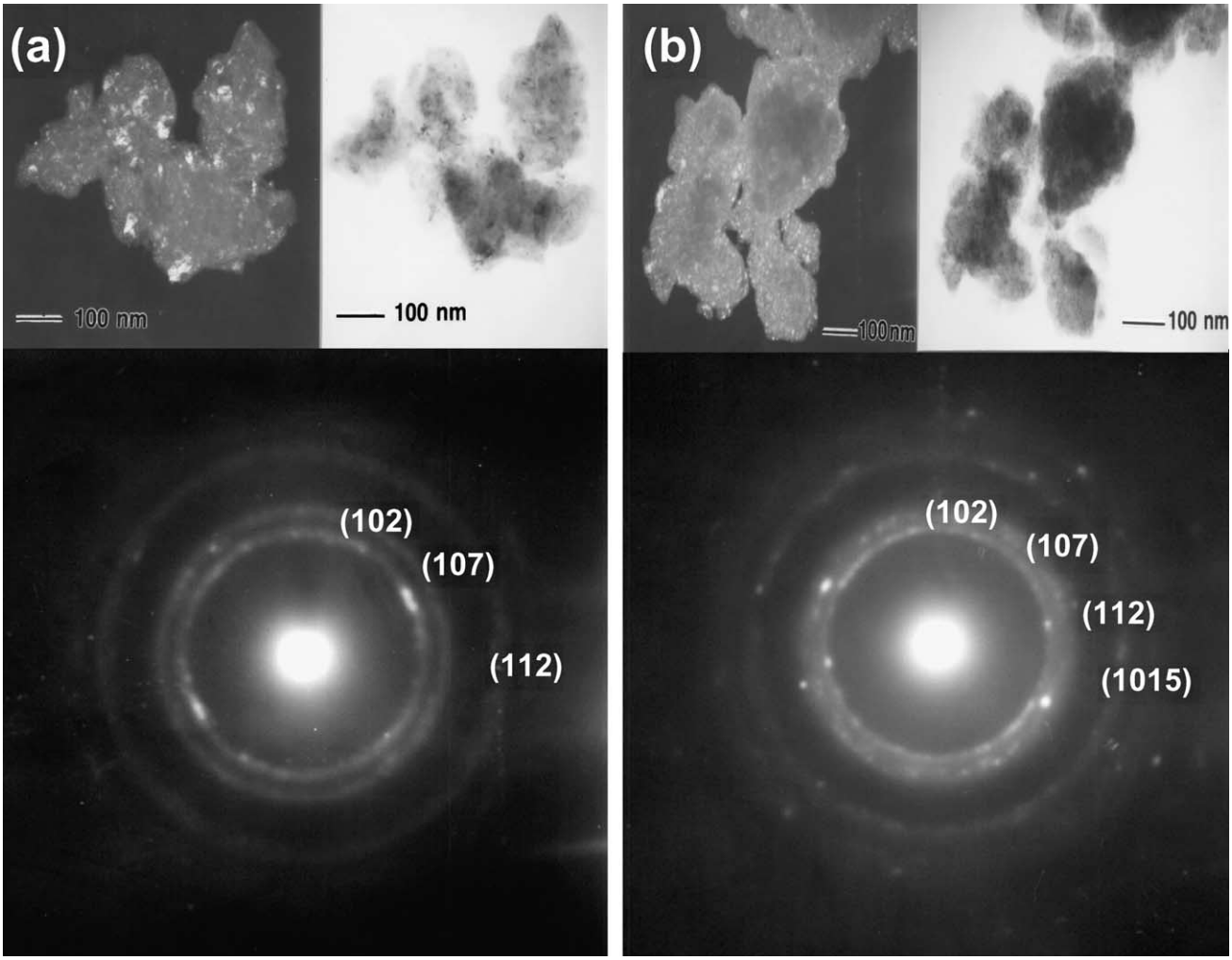

Fig. 5. TEM micrographs (bright and dark field images) and SAD pattern of: (a) Ti–5 wt.% Al and, (b) Ti–30 wt.% Al ball milled for 16 h by IRBM, both showing nanoparticles of the Ti–Al alloy.

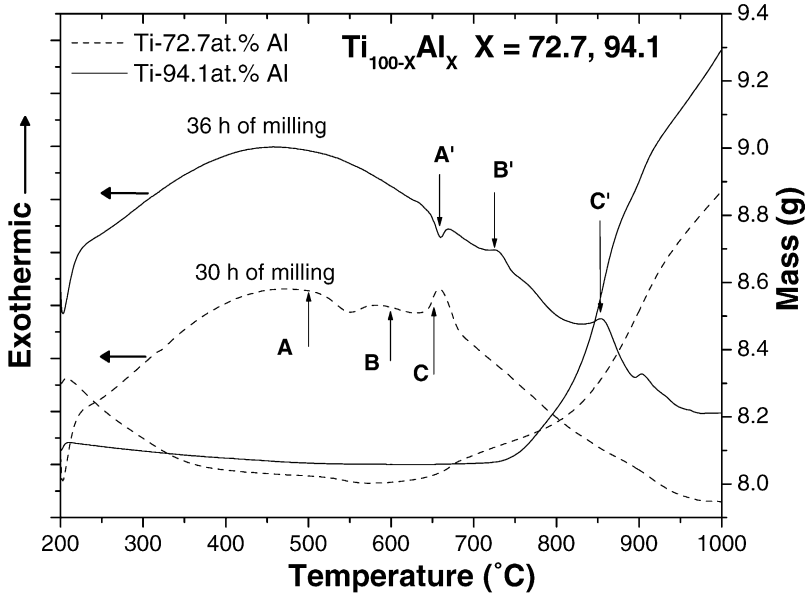

Fig. 6. DTA and TGA curves of Ti–72.7 at.% Al and Ti–94.1 at.% Al powders ball milled by IRBM for 30 and 36 h of milling, respectively.

of mechanically alloyed Ti–Al powders with 75 at.% of Al in Ar-atmosphere, in order to prepare Al_3Ti. After milling times of 40 h a nanocrystalline alloy of Al(Ti) was prepared, which was thereafter heat treated by 800 and 900 °C to successfully prepare $D0_{22}$-Al_3Ti. Calderón et al. [21] used MA experiments to produce nanocrystalline powders of Ti–Al–X (X = Cr, Fe, Mn) intermetallic alloys getting particle sizes in the range of 120–280 nm milling as long as 700 h in high energy horizontal ball mills. We conclude that the proposed IRBM process offers a higher efficiency in powder size reduction and high energy MA compared to the RBM or conventional high energy MA process.

Fig. 5 shows TEM micrographs (bright and dark field images) and the correspondent selected area diffraction (SAD) patterns of Ti–5 wt.% Al and Ti–30 wt.% Al powders, which were ball milled for 16 h by IRBM both showing nanoparticles of the Ti–Al alloy. The grain size observed from the dark field image was less than 20 nm, which confirms our results from the Warren–Averbach analysis of the XRD patterns. TEM results reported elsewhere by Moon and Lee [17] showed the tendency of multimodal particle distributions from the multiple components of the milled powder. For instance, Moon and Lee [17] observed differences in pure Al powders SAD pattern showed that the area con-

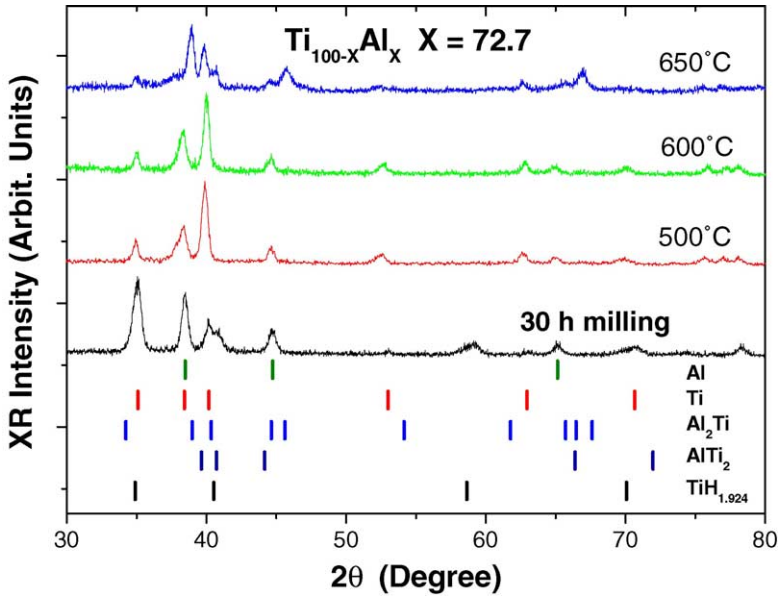

Fig. 7. XRD patterns of Ti–72.7 at.% Al (Ti–60 wt.% Al) powders ball milled by IRBM for 30 h of milling and heated to various temperatures.

sisted of $TiH_{1.924}$, Ti(Al), and in some cases Al(Ti), TiN or Al_3Ti.

3.2. Thermal stability of the powders

As mentioned before, the light metal hydrides are unstable at temperatures higher than 250 °C. By doing the characterization of thermal stability of the powders we were able both to eliminate the hydride compound from the powders and to confirm their formation during the IRBM process. Additionally, we were interested in studying the structural evolution of the powders during the heat treatment in order to identify intermetallic phases.

Fig. 6 shows the TG–DTA curves (dashed lines) for the sample Ti–72.7 at.% Al (Ti–60 wt.% Al) after 30 h of milling, measured in a nitrogen flux with a heating rate of 10.0 °C/min. Simultaneously, structural changes of the milled and subsequently annealed sample were analyzed by XRD measurements. TG curve shows a mass decreasing associated with the desorption of hydrogen and some volatile species from 8.32 g at 200 °C until 8.00 g at 600 °C, approximately 3.8 wt.%. Above 700 °C, in TG curve, an increasing of mass, possibly due to absorption of nitrogen from the atmosphere of the measurement system to form Ti or Ti(Al) nitrides is observed. DTA curve in the range from 300 to 700 °C shows three exothermic events (points A, B and C, respectively). The first exothermic peak (A) with a maximum at 474.1 °C, is due to the hydrogen desorption and to a structure reordering such as the formation of some crystalline phase of Ti(Al) solid solution. The event between 550 and 700 °C is associated with the formation of the crystalline phase of Al_2Ti (long period superstructure), as was proved by XRD measurements. The next phase transformation was identified as an endothermic event at about 658 °C corresponding to the aluminum fusion. This sample was annealed by 1 h in a continuous argon flux at the temperatures of 500, 600 and 650 °C; close to the points A, B and C of this figure. Fig. 7 shows the XRD patterns obtained from the sample Ti–72.7 at.% Al (Ti–60 wt.% Al) as prepared after 30 h of milling and annealed at mentioned temperatures. After annealing at 500 °C the diffraction pattern shows a decomposition of the (Ti, Al)H compound into Ti(Al) solid solution. It is not surprising that at this temperature there is not signal from titanium hydride, which is due to hydrogen desorption as was observed in the TGA curve. After annealing at 600 °C the diffraction pattern does not show significant changes respective to the sample annealed at 500 °C. The thermal stability of the mixture apparently was not affected by the temperature near the aluminum fusion. However, for annealing at 650 °C, a clear change is shown in the diffractogram, where crystalline phase of Al_2Ti is identified. On the other side, low intensity and broadened peaks from Al or Ti(Al) phase are still observed. We assume that two exothermic events (B and C) are taking place; one corresponds to the formation of Al_2Ti phase, which is maintaining a compromise with a second endothermic event, fusion of remnant aluminum. This behavior can be described by the next relation:

$$\begin{aligned} &TiH_{1.924} + Al(Ti) + Ti \\ &\xrightarrow{500\,^{\circ}C} Ti(Al) + Al + H_2 \uparrow Ti(Al) + Al \\ &\xrightarrow{650\,^{\circ}C} Ti + Al_2Ti + Al \end{aligned} \tag{3}$$

TG–DTA curves from the sample Ti–94.1 at.% Al (Ti–90 wt.% Al) after 36 h of milling time are shown also in Fig. 6 (solid lines). For this sample the Ti content is low, and consequently its capacity to form $TiH_{1.942}$ is limited, as already shown by the TG curve. The loss of mass in the range

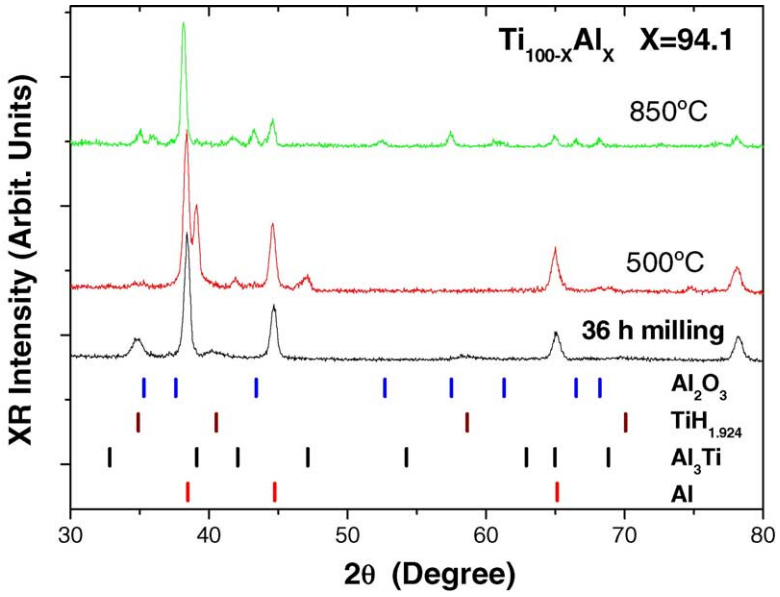

Fig. 8. XRD patterns of the Ti–94.1 at.% Al (Ti–90 wt.% Al) powders ball milled by IRBM for 30 h of milling and heated to various temperatures.

from 200 to 600 °C due to hydrogen desorption is less than 0.1 g (∼0.9 wt.%). The DTA curve does not show notable thermal events before 600 °C, except a wide exothermic peak centered at about 450 °C. This released energy is associated with both mass loss and reordering events of the system. For higher temperatures, three events are marked: an endothermic (point A′, 659 °C) and two exothermic events (point B′, 726 and C′, 853 °C). Point A′ corresponds to fusion of Al, while B′ and C′ are phase transformations that can be understood from XRD measurements on annealed samples as shown in Fig. 8. This figure was constructed with plots of diffractograms obtained with samples annealed at 500 and 850 °C by 1 h under argon atmosphere. The plot of the sample "as prepared" defines the presence of $TiH_{1.942}$ and Al(Ti) phases, while the patterns for the sample annealed at 500 °C showed peaks of elemental Al and the intermetallic Al_3Ti that can be formed according to the next reaction:

$$TiH_{1.924} + Al(Ti) \xrightarrow{500\,^{\circ}C} Al_3Ti + Al(Ti) + H_2 + \uparrow Al_3Ti + Al(Ti) \xrightarrow{850\,^{\circ}C} Al_2O_3 + Al(Ti) \quad (4)$$

XRD results for the sample annealed at 850 °C proved that some oxygen is absorbed by Al to form Al_2O_3 in addition to formation of the intermetallic Al_3Ti with respect to the sample annealed at 500 °C. Oxygen absorption could occur due to the reaction of powders with residual oxygen in the annealing atmosphere. Thus, the exothermic peaks B′ and C′, in Fig. 8, can be associated with the phase transformation needed to form intermetallic Al_3Ti and Al_2O_3, respectively.

4. Conclusions

Indirect reactive ball milling was successfully applied to obtain different nanocrystalline and amorphous powder alloys of the Ti–Al binary system. The effect of the milling time on the structural evolution and thermal stability of the samples was studied. A $TiH_{1.924}$ phase was invariably detected by XRD in all compositions even after 4 h of milling by IRBM. We confirmed that the in situ formation of titanium hydride material lead to an efficient and effective grain size reduction in the samples regardless of the aluminium content during milling. Compositions with Al contents less than $x \leq 43.2$ at.% showed faster grain size reduction. The grain size observed from TEM micrographs and confirmed with the profile analysis of XRD patterns was less than 15 nm after very short milling times (4 h) and less than 5 and 10 nm for alloys with low (milled by 8 h) and high Al contents (milled by 36 h), respectively. Samples with high Ti content need special care after milling, due to the high reactivity of the powders of $TiH_{1.924}$ and Ti(Al) when they are exposed to nitrogen and oxygen atmosphere. The corresponding TiN contaminant formation was detected when the powders were exposed to the ambient environment.

For the maximum milling time, about 36 h, samples with high Al content were amorphous or nanostructured with a crystalline grain less than 10 nm embedded in an amorphous matrix. DTA and TGA results showed the hydrogen desorption and some structure reordering in the temperature range of 200 to 600 °C. As temperature increased, amorphous and/or metastable phases changed to more stable phases such as Al_2Ti and Al_3Ti intermetallic compounds.

Acknowledgements

This work was supported by CONACYT under the research project G33178-U, and partially by CONCyTEQ (Querétaro, México). The authors recognize the helpful participation of L.L. Díaz Flores, M.A. Hernández Landaverde, R. Flores Farías, M.C. Delgado Cruz, J.E. Urbina Alvarez, and R. Martinez (CIMAV).

References

[1] R. Janot, A. Rougier, L. Aymard, C. Lenain, R. Herrera-Urbina, G.A. Nazri, J.M. Tarascon, J. Alloys Compd. 438 (2003) 356.
[2] C. Suryanarayama, Prog. Mater. Sci. 46 (2001) 1.
[3] P.L. Martin, D.A. Hardwick, in: J.H. Westbrook, R.L. Fleischer (Eds.), Intermetallic Compounds, Wiley, New York, 1994, p. 637.
[4] A. Takasaki, Y. Furuya, Nanostruct. Mater. 11 (1999) 1205.
[5] T. Itsukaichi, K. Masuyama, M. Umemoto, I. Okane, J.G. Cabanas-Moreno, J. Mater. Res. 8 (1993) 1817.
[6] M. Oehring, T. Klassen, R. Bormann, J. Mater. Res. 8 (1993) 2819.
[7] K.Y. Wang, J.G. Wang, G.L. Chen, J. Mater. Res. 10 (1995) 1247.
[8] S. Orimo, H. Fujii, T. Yoshino, J. Alloys Compd. 217 (1995) 287.
[9] T. Fuji, M. Kuzutani, N. Nakabo, K. Ameyama, J. Jpn. Inst. Met. 62 (1998) 462.
[10] A. Calka, J.S. Williams, Mater. Sci. Forum 88 (1992) 787.
[11] D.L. Zhang, D.Y. Ying, Mater. Lett. 50 (2001) 149.
[12] T. Itsukaichi, S. Shiga, K. Masuyama, M. Umemoto, I. Okane, Mater. Sci. Forum 88 (1992) 631.
[13] J.S. Benjamin, M.J. Bomford, Metall. Trans. 8A (1977) 1301.
[14] N. Burgio, W. Guo, M. Magín, F. Padella, F. Martelli, I. Soletta, Proc. ASM Int. Conf. Struct. Appl. Mech. Alloying (1990) 175.
[15] K. Hashi, K. Ishikawa, K. Suzuki, K. Aoki, J. Alloys Compd. 330 (2002) 547.
[16] F.J. Espinoza-Beltrán, O. Ceh-Soberanis, L. García-González, J. Morales-Hernández, Thin Solid Films 437 (2003) 170–175.
[17] K.I. Moon, K.S. Lee, J. Alloys Compd. 264 (1998) 258.
[18] K.I. Moon, H.S. Park, K.S. Lee, J. Alloys Compd. 325 (2001) 236.
[19] A. Takasaki, Y. Furuya, Nanostruct. Mater. 11 (1999) 1205.
[20] F. Zhang, L. Lu, M.O. Lai, J. Alloys Comp. 297 (2000) 211.
[21] H.A. Calderón, V. Garibay-Febles, A. Cabrera, M. Umemoto, J.G. Cabañas-Moreno, K. Tsuchiya, Mater. Res. Soc. Symp. Proc., vol. 552, 1999, Materials Research Society, KK5.6.1.